Influence of mechanical strain in Si and Ge p-type double gate MOSFETs

M. Moussavou*, N. Cavassilas, E. Dib and M. Bescond
IM2NP, UMR CNRS 7334, Marseille, France
Email: manel.moussavou@im2np.fr

***Abstract*—We theoretically investigate the impact of uniaxial strain in extremely thin Si and Ge p-type double gate transistors. Quantum transport modeling is treated using a 6-band k.p Hamiltonian and the non-equilibrium Green's function formalism including hole-phonon scattering. Based on this framework we analyze the influence of strain on current characteristics considering different transport directions and gate length's. The results first confirm the dominance of Ge in long devices (15 nm gate length) for which best electrical performances are obtained for channels along $< 110 >$ with a uniaxial compressive strain. Situation is reversed for shorter devices (7 nm gate length) where the small effective masses of Ge deteriorate the off-regime of transistors regardless the considered strain. Due to weaker hole-phonon scattering, $< 100 >$ Si devices with a tensile strain are interestingly found to be more competitive than their $< 110 >$-compressive counterparts.**

I. Introduction

Reduction of transistor size is required to continue the growth of semi-conductor industry. Strain engineering has been introduced since the 90 nm node as a technological booster to maintain the improvement of performances of Si-CMOS transistors [1]. For instance, it is generally admitted that uniaxial tensile strain for Si nMOSFETs and uniaxial compressive strain for Si pMOSFETs represent the best strategy to enhance the transistor performances [2]. An additional solution is to consider multi-gate transistors to improve the electrostatic control of the channel potential [3]. More recently, Ge channel material has been envisaged as another booster of holes mobility [4], [5]. In that context a careful analysis of the influence of channel material, strain and crystallographic orientation is essential to fully assess the potentialities of nano-transistors. The issue is even more complicated when considering p-type devices since both multiband nature of valence-band and hole-phonon scattering may have a substantial impact on current characteristics [6]. As a consequence, only realistic multi-band quantum simulations are able to clearly settle the most suitable strain configuration for a given p-type architecture.

In this work we then propose a theoretical study of p-type double-gate Si- and Ge-based MOSFETs for various strain options, channel orientations and channel length's. We use the non-equilibrium Green's function (NEGF) formalism expressed within the six-band k.p Hamiltonian. Acoustic- and optical-phonon scatterings are addressed within the self-consistent Born approximation [7], [8]. Strain is handled through the Bir-Pikus Hamiltonian.

This work is organized as follows: Section II presents the general theoretical framework while section III discusses the influence of uniaxial strain as a function of the channel length, material and crystallographic orientation. The impact of hole-phonon scattering is particularly emphasized. Section IV summarizes the key findings.

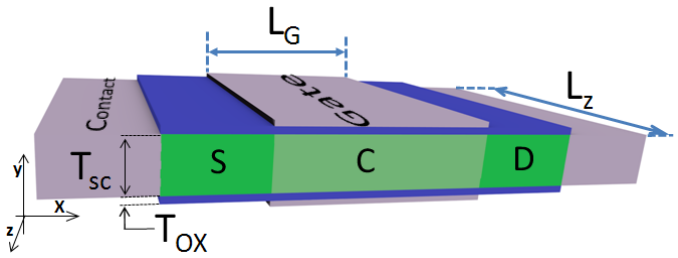

Fig. 1. Top view of the considered Double-Gate p-type MOSFETs. For all devices T_{SC}=2 nm, T_{OX}=1 nm, Source and Drain doping is 10^{20} cm^{-3} and L_G equals to 15 or 7 nm and V_{DS}= -0.4 V.

II. Method

We use the NEGF transport equations expressed within the 6-band k.p Hamiltonian to implement a 2D real-space self-consistent simulator. The 2D k.p Hamiltonian discretization is performed by replacing the wave vector $\overrightarrow{k_\xi}$ such that $\mid \overrightarrow{k_\xi} \mid \longrightarrow -i\partial/\partial\xi$, where $\xi = x, y$, respectively correspond to the transport and confinement directions [9]. The discretization is then made using a finite difference scheme. The wave vector along the z direction, $\overrightarrow{k_z}$, takes into account transverse-modes. Born-Von-Karman periodic boundary conditions are applied to the $\overrightarrow{k_z}$ wave vector component such that $k_z(t) = 2\pi t/L_z$, with L_z=20 nm the device finite size along the z direction and t an integer describing the indice of the transverse modes. Up to 10 discrete values of transverse modes are added up to ensure accurate calculations. Acoustic- and optical-phonon interactions are addressed within the self-consistent Born approximation (SCBA) based on interaction self-energy concept [9] [10]. Stress/strain is handled by calculating strain tensor for each strain configuration. The Bir-Pikus strain Hamiltonian is calculated using the resulting strain tensor and added up to the 6-band k.p Hamiltonian incorporating the spin-orbit coupling. Strain effects and phonon scattering are described through the Bir-Pikus deformation-potential theory taking bulk values of deformation potentials. All parameters used in our approach are shown in TABLE I and are extracted from refs [11], [12].

III. Simulation results and discussion

Fig. 1 represents the considered double-gate p-type transistor: the channel and SiO_2 gate oxide are 2 nm and 1 nm thick

978-1-4673-7860-4/15/$31.00 ©2015 IEEE

TABLE I. PRINCIPAL MATERIAL PARAMETERS USED IN THIS WORK FOR Si AND Ge.

		Si	Ge
Luttinger parameters	γ_1	4.285	13.35
	γ_2	0.339	4.25
	γ_3	1.446	5.69
Spin orbit splitting (meV)	Δ	44	296
Deformation potentials (eV)	a	2.45	1.17
	b	-2.1	-2.9
	d	-4.8	-5.3
	d_0	37.9	29.1
Optical-phonon energy (meV)	$\hbar\omega$	63	37

respectively. The source and drain regions are p-doped with an acceptor concentration of $N_A = 10^{20}$ cm^{-3}. Based on the methodology presented in the previous section, we compare Si and Ge p-type DG transistors made on (001) oriented wafers with a channel direction along $< 100 >$ and $< 110 >$. In order to emphasize the modifications of the transport properties in ultimate transistors, two channel length's $L_G = 15$ nm and 7 nm are studied. All calculations are performed with a source-drain bias $V_{DS} = -0.4$ V.

In Fig. 2 we show the impact of strain on the band structure by comparison of the unstrained case (Fig. 2**a**) with the compressive strain for the two transport directions. We observe that subband curvature modifications are more important along the $< 110 >$ (Fig. 2**b**) than in the $< 100 >$ direction (Fig 2**c**). This remark is also valid considering tensile strain. In order to have a better estimation of strain effect on band structure, we present in TABLE II the effective mass values exctracted from the top of the first valence subband for the most populated transverse mode $k_z = 0$ nm^{-1}. We notice that similar behaviors are obtained with Ge and Si such that hole effective masses are increased by a $< 110 >$-tensile stress and are reduced by a $< 110 >$-compressive one. The lowest effective masses are obtained with Ge especially when considering $< 110 >$-Ge compressive strain ($m^* = 0.048 \times m_0$).

TABLE II. EFFECTIVE MASS VALUES ($\times m_0$) EXTRACTED FROM THE TOP OF THE FIRST SUB-BAND FOR THE FIRST TRANSVERSE MODE.

	Si	Ge
$< 110 >$ direction		
Unstrained	0.295	0.078
Comp.	0.163	0.048
Tens.	2.951	0.178
$< 100 >$ direction		
Unstrained	0.327	0.076
Comp.	0.295	0.152
Tens.	0.281	0.051

Based on ITRS off-current requirements, we analyze the current characteristics for different strain options by extracting the drive current according to the V_{DS} value. Fig 3 presents

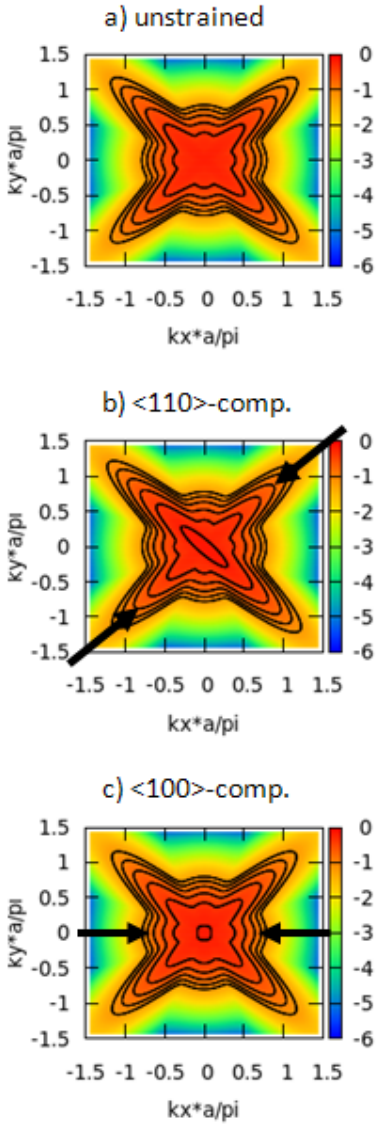

Fig. 2. k_x-k_z mapping of the first Si valence band for the different applied strains (±2 GPa): a) relaxed, b) compressive strain along $< 110 >$, c) tensile along $< 100 >$.

I_{OFF} *vs* I_{ON} curves for Si- and Ge-based devices with $L_G = 15$ nm in the ballistic regime. These results clearly express the effective mass dependence of the drive current: **i**) currents obtained with strained $< 100 >$ oriented devices are almost similar to the unstrained case due to the $< 100 >$ weaker strain sensitivity, **ii**) $< 110 >$-compressive Ge based device is found to provide best electrical performances due to its lowest effective mass.

Hereinafter hole-phonon scattering will be included in simulations. Fig. 4 shows that for 15 nm gate length, hole-phonon scattering does not change the performance ranking obtained in the ballistic situation and are in agreement with previous studies [13], [14].

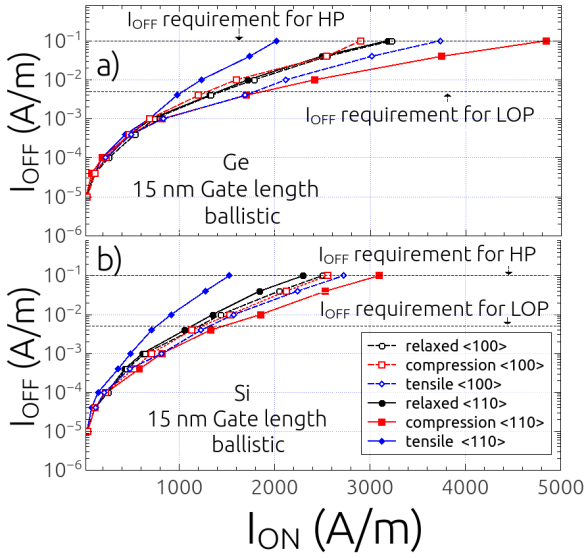

Fig. 3. I_{OFF} *vs* I_{ON} curves for **a)** Ge-based and **b)** Si-based 15 nm gate length MOSFETs in the ballistic regime. I_{ON} is extracted with respect to the ITRS high-performance (HP) and low operating power (LOP) off-current requirements and according to the V_{DS} value .

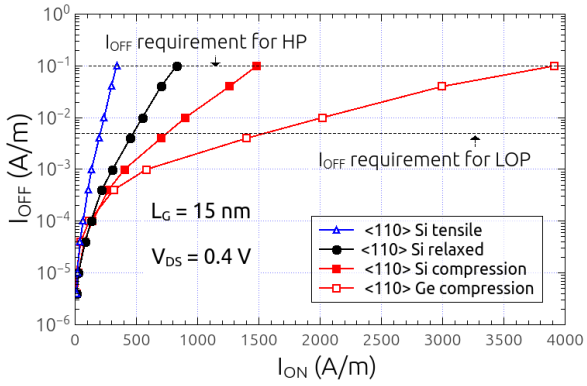

Fig. 4. I_{OFF} *vs* I_{ON} curves considering hole-phonon scattering for 15 nm gate length devices .

Situation is significantly modified when reducing L_G. Fig. 5 shows the equivalent I_{OFF} *vs*. I_{ON} curves at $L_G = 7$ nm for various strain options in Ge based devices. The small effective masses and the weak hole-phonon coupling of Ge are now detrimental and correspond to a strong tunneling effect through the channel potential barrier.

Fig. 6 shows $I_D - V_G$ characteristics for Ge devices along $< 100 >$ in which the effective mass influence on the subthreshold slopes is clearly visible. For this material the $< 100 >$-compression provides the best current characteristics since it generates the largest effective mass. On the other hand Si devices offer much better current characteristics due to larger effective masses (Fig. 7). The best performances are now obtained along $< 100 >$-direction whose intermediate effective masses provide both a good control of the off regime and a rather high on-current. In particular optimum current is delivered by the $< 100 >$-tensile configuration which now

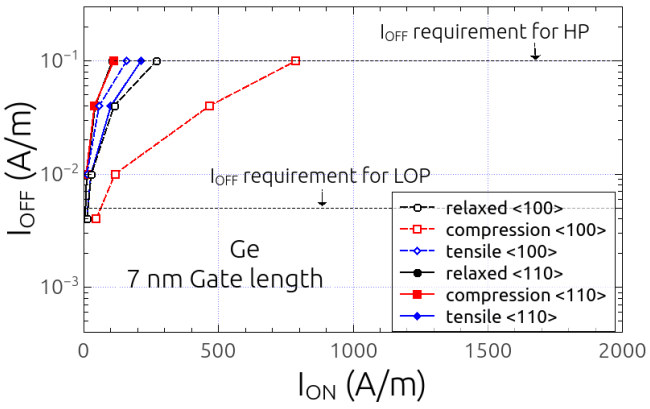

Fig. 5. Targeted I_{OFF} *vs*. I_{ON} curves for Ge-based devices for all the strain options. $L_G = 7$ nm. The dashed lines represent the ITRS targeted I_{OFF} values for high power (HP) and low operating power (LOP) device requirements.

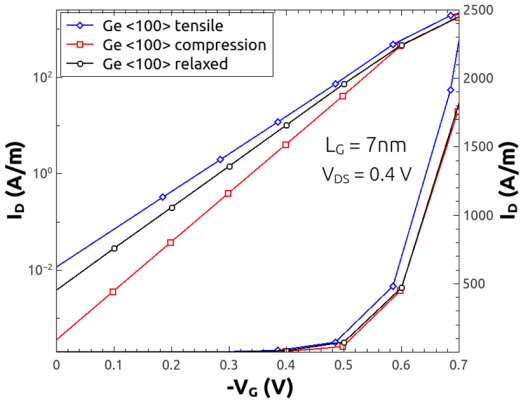

Fig. 6. $I_D - V_G$ characteristics for Ge p-type double-gate transistor along the $< 100 >$ direction for three strain options: tensile (diamonds), compression (squares) and relaxed (circles). $L_G = 7$ nm. Phonon scattering is included in the simulations.

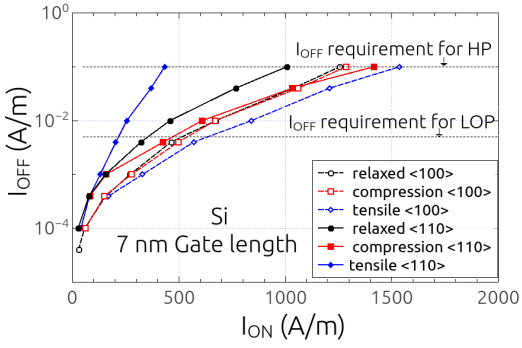

Fig. 7. I_{OFF} vs. I_{ON} curves for Si-based devices for the various strain options. $L_G = 7$ nm. The dashed lines represent the ITRS targeted I_{OFF} values for high power (HP) and low operating power (LOP) device requirements. Phonon scattering is included in the simulations.

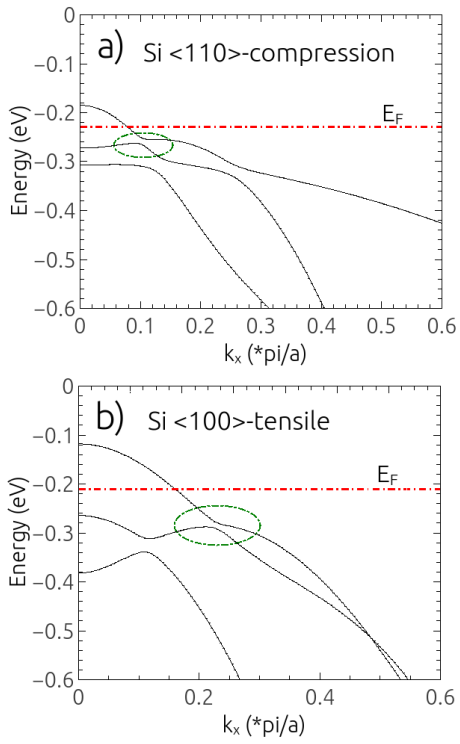

Fig. 8. First three sub-bands of the Si valence band for the first transverse mode $k_z = 0\ nm^{-1}$: **a**) $< 110 >$-compressive strain situation and **b**) $< 100 >$-tensile strain one. The dashed line represent the Fermi level E_f. Arrows indicate anti-band crossing .

surpasses its $< 110 >$-compression counterpart. This result is explained by band structure and hole-phonon scattering considerations. Indeed $< 110 >$-compression suffers from a stronger hole-phonon scattering than the $< 100 >$-tensile case. As an illustration, Fig. 8 shows band structure of the first transverse mode in wich we notice that band anti-crossing is closer to the Fermi level in the case of $< 110 >$-compression which is then more damaging for the current. Note that for 7 nm gate length, tensile strain is found to be the worst solution along $< 100 >$ direction in the ballistic regime, demonstrating the importance of hole-phonon scattering in ultra scaled transistors.

IV. Conclusion

In this work the influence of uni-axial strain in p-type Si and Ge DG transistors has been analyzed for different channel orientations and length's. Based on a 2D real space non-equilibrium Green's function code expressed within a 6-band k.p Hamiltonian, we confirm that $< 110 >$ compressive Ge devices are the most relevant choice for long channel length L_G=15 nm. Material supremacy is reversed when reducing the gate length to 7 nm. Indeed the small effective masses of Ge now generates high tunneling current for all strain and crystallographic options. For short gate length, Si remains a good solution as a channel material but the usual $< 110 >$-compression option suffers from strong hole-phonon scattering. Interestingly Si devices with tensile strain along $< 100 >$ provide the best electrical properties, giving a remarkable opportunity to consider the same tensile strain for both n-type and p-type Si planar devices at the far end of the ITRS.

Acknowledgment

This work was supported by the NOODLES project funded by the ANR-French National Research Agency

*) Corresponding author - electronic address: manel.moussavou@im2np.fr

References

[1] S. Thompson, N. Anand, M. Armstrong, C. Auth, B. Arcot, M. Alavi, and P. Bai, *Proc. IEEE IEDM*, vol. 46, p. 61, 2002.

[2] S. W. Bedell, A. Khakifirooz, and D. Sadana, *MRS Bulletin.*, vol. 39, p. 131, 2014.

[3] J. Colinge, *Solid States Electron.*, vol. 48, p. 897, 2004.

[4] K. C. Saraswat, C. O. Chui *et al.*, *Proc. IEEE IEDM*, p. 659, 2006.

[5] K. Kuhn, *IEEE Trans. Electron Devices*, vol. 59, p. 1813, 2012.

[6] N. Cavassilas, F. Michelini, and M. Bescond, *J. Appl. Phys.*, vol. 109, p. 073706, 2010.

[7] A. Svizhenko and M. P. Anantram, *IEEE Trans. Elec. Dev.*, vol. 50, p. 1459, 2003.

[8] M. Luisier, *App. Phys. Lett.*, vol. 98, p. 032111, 2011.

[9] N. Cavassilas, F. Michelini, and M. Bescond, *J. Appl. Phys.*, vol. 109, p. 073706, 2011.

[10] M. Bescond, C. Li, and H. M. et al, *J. Appl. Phys.*, vol. 114, p. 153712, 2013.

[11] J. M. Hinckley and J. Singh, *Phys. Rev. B*, vol. 41, p. 2912, 1990.

[12] C. Jacoboni and L. Reggiani, *Rev. Mod. Phys.*, vol. 55, p. 645, 1983.

[13] T. Krishnamohan, D. Kim, T. Dinh, A. Pham, B. Meinerzhagen, C. Jungemann, and K. Saraswat, *Proc. IEEE IEDM*, p. 1, 2008.

[14] S. Gupta, V. Moroz, L. Smith, Q. Lu, and K. Saraswat, *IEEE Trans. Electron Devices*, vol. 61, p. 1222, 2014.